IN SITU, 20(2), 115–135 (1996)

GELANT PLACEMENT IN ANISOTROPIC FLOW SYSTEMS

Mei Ye and Randall S Seright
New Mexico Petroleuin Recovery Research Center
New Mexico Institute of Mining and Technology
Socorro. New Mexico 87801

ABSTRACT

This paper is coiicemed with the proper placement of gels to reduce fluid channeling in reservoirs. Previous work demonstrated that an acceptable gel placement is much more likely to be achieved in a linear flow geometry (e.g., vertically fractured wells) than in radial flow. In radial flow, oil-productive zones must be protected (e.g., using zone isolation) during gel placeineiit to prevent damage to oil productivity. hi this study. two theoretical models were developed to determine water injection profiles before and after gel placement in anisotropic reservoirs — where the effective permeability and/or the pressure gradient are greater in one horizontal direction than in another direction. The primary question addressed in this work is, how anisotropic must an unfractured reservoir be to achieve an acceptable gel placement and profile modification during unrestricted gelant injection? Both analytical and numerical methods were applied to solve the problem. We studied how the effectiveness of gel treatments is influenced by permeability variation, distance of gelant penetration, anisotropic pressure distributions, resistance factor, and residual resistance factor.

Our analyses showed that the range of pernieability variations (pemieability in the most-permeable direction divided by pemieability in the least-peniieable direction) must be greater than 1,000 (and usually greater than 10,000) before anisotropy caii be exploited to achieve a satisfactory gel placement in unfractured wells We doubt that any unfractured wells or reservoirs exist with this degree of anisotropy hi contrast, in wells and reservoirs where anisotropic flow is due to fractures, the linear flow geometry and the extreme permeability contrast between the fracture and the porous rock can aid gel placement substantially

INTRODUCTION

. Gels have frequently been used to improve conformance in reservoirs.[1] A critical issue when applying gels for this purpose is how to place gels in the high-permeability water channels without damaging the less-penneable, oil-productive zones. Previous work demonstrated that an acceptable gel placement is much more likely to be achieved in a linear flow geometry (e.g., vertically fractured wells) than in radial flow.[4-8] In radial flow, oil-productive zones **must** be protected (e.g., using zone isolation) during gel placement to prevent damage to oil productivity.

In the analysis of gel placement to date, only linear and purely radial flow geometries were considered. However, flow **in** reservoirs is often anisotropic—the effective penneability and/or the pressure gradient are greater in one horizontal direction than in another direction. Anisotropic flow can occur in both fractured and unfractured reservoirs.[9] In the naturally fractured Spraberry field, Elkins and Skov[10] reported that the effective reservoir permeability along the main fracture trend is 13 times greater than that at right angles to this trend. As expected,[9] penneability anisotropy is significantly less in unfractured reservoirs. For example, Ramey[11] reported only a 56% permeability anisotropy for a channel-sand reservoir (i.e., k_x/k_y=1.56).

In fractured reservoirs, gel placement can be effectively treated as a linear flow problem.[12] However, unfractured anisotropic reservoirs can be viewed as flow geometries that are intermediate cases between linear and radial flow. In fact, a linear flow geometry can represent the extreme case of an anisotropic reservoir. Since the requirements for **an** effective gel placement are radically different for linear vs. purely radial flow, questions arise about gel placement during anisotropic flow in unfractured reservoirs: How anisotropic must an unfractured reservoir be to allow gelant placement to approximate that for the linear flow case? Asked another way, how anisotropic must an unfractured reservoir be to achieve an acceptable gel placement during unrestricted gelant injection? These questions will be addressed here by developing two models of simple anisotropic flow systems and by performing sensitivity studies with these models.

MODELS USED

To illustrate how areal flow profiles in an anisotropic reservoir are modified by a gel treatment, two circular theoretical reservoir models were used. Model 1 was established in a Cartesian coordinate system by aligning the x-axis with the most-

permeable horizontal direction while aligning the y-axis with the least-permeable horizontal direction. The origin coincided with the center of the reservoir. An injection well was located in the center of the reservoir, and flow was produced at the outer boundary of the reservoir. Both the injection well and the outer boundary of the reservoir were assigned a constant pressure.

In Model 2, an isotropic reservoir having the same dimensions was considered. The pressure distribution was symmetrical about both the x-axis and the y-axis, and only the injection well was assigned a constant pressure. The reservoir experienced the largest pressure drop in the x-direction while the smallest pressure drop occurred in the y-direction.

ANALYSIS USING MODEL 1

Streamlines

In Model 1, both the inner boundary (injection wellbore) and the outer drainage boundary are circular equipotential lines. Therefore, the equipotential curves in the drainage area should also be concentric circles. Since streamlines are always perpendicular to the equipotential curves, the streamlines in the drainage area must be radial. Therefore, the key to the solution of this problem is to determine an expression for the permeability distribution and the relationship between the distance of gelant penetration and the fluid and reservoir properties.

Permeability Distribution

Permeabilities in any radial direction between the x-axis and the y-axis are given by Eq. 1 (which is derived in Appendix B of Ref. 13. *).

$$k_i = \frac{1}{\frac{\cos^2\theta_i}{k_x} + \frac{\sin^2\theta_i}{k_y}} \qquad (1)$$

where

* Ref. 13 can be obtained from the National Technical Information Service, U.S. Department of Comnerce, 5285 Port Royal Rd., Springfield VA 22161

k_i = permeability in a given radial direction, md
k_x = permeability in the most-permeable direction (x-direction), md
k_y = permeability in the least-permeable direction (y-direction), md
θ_i = the angle between the considered radial direction and the x-axis

Areal Flow Profile During Gelant Injection

Eq. 2 can be used to find the distance of gelant penetration in any radial direction.

$$\frac{\phi_i}{k_i}\left\{r_{pi}^2\left[F_r \ln\left(\frac{r_{pi}}{r_w}\right)+\ln\left(\frac{r_e}{r_{pi}}\right)+\frac{(1-F_r)}{2}\right]-r_w^2\left[\ln\left(\frac{r_e}{r_w}\right)+\frac{(1-F_r)}{2}\right]\right\}=\text{Constant} \qquad (2)$$

where

F_r = resistance factor (brine mobility before gelant placement divided by gelant mobility)
r_e = radius of the outer boundary, ft
r_{pi} = distance of gelant penetration in a given radial direction i, ft
r_w = radius of the injection wellbore, ft
ϕ_i = effective porosity in radial direction i

Eq. 2 is derived in Appendix C of Ref. 13 and assumes the following.

1. Fluids are incompressible and Newtonian.
2. The displacement is miscible and piston-like.
3. Dispersion, adsorption, and gravity effects are negligible.
4. The pressure drop between the injection well and the outer boundary is constant.
5. Only aqueous fluids are mobile in the reservoir.
6. The drainage area is circular.
7. The resistance factor is independent of permeability.
8. The same effective Permeability applies to the displacing and displaced fluids.

The areal flow profiles of the gelant front when gelant reaches the outer boundary in the x-direction are shown in Fig. 1, which was generated assuming (1) $r_w = 1/3$ ft, (2) $r_e = 50$ ft, (3) $\phi_i = 0.2$, and (4) $F_r = 1$. Fig. 1 shows that, as expected, the areal flow profile in this anisotropic reservoir becomes less favorable as k_x/k_y increases.

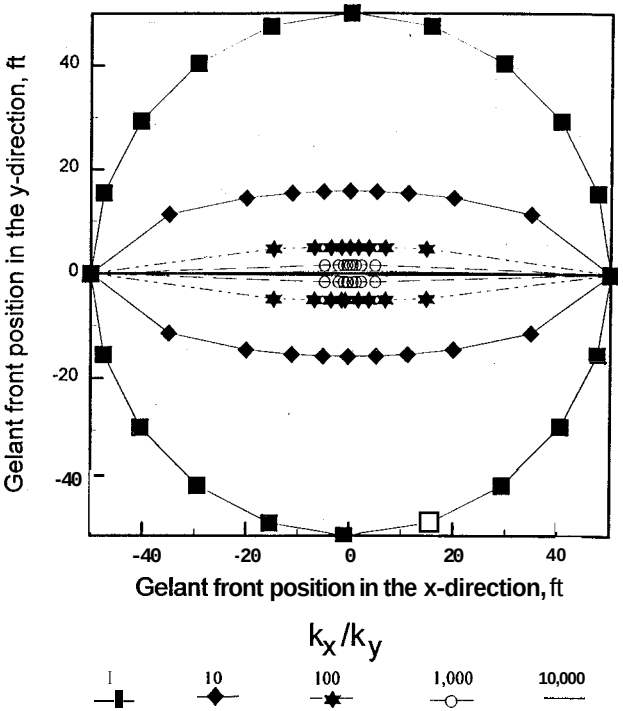

FIG. 1. Plan view of the gelant front. $F_r = 1$.

Effect of Resistance Factor

Fig. *2* plots the degree of gelant penetration (the distance of gelant penetration in direction i divided by the distance of gelant penetration in the x-direction) against permeability ratio (k_x/k_i) when gelant reaches the outer boundary in the x-direction. Consistent with the observations reported in Ref. **4,** Fig. 2 shows the following.

1. For a given permeability ratio, the degree of gelant penetration, $(r_{pi}-r_w)/(r_{px}-r_w)$, increases with increased resistance factor.
2. For the range of permeability variations investigated ($k_x/k_i \leq 10^6$), the degree of gelant penetration is insensitive to resistance factor for $F_r \geq 100$.
3. For a given permeability ratio, the degree of gelant penetration is greater in anisotropic radial flow than in linear flow.

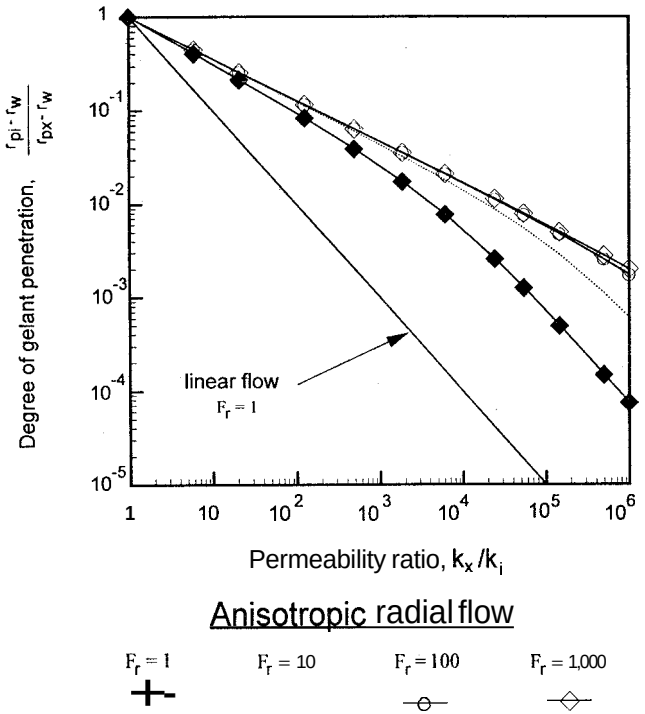

FIG. 2. Degree of gelant penetration in direction i vs. permeability ratio when gelant reaches the outer boundary in the most-permeable direction.

Iniectivitv Expressions

Injectivity loss in a well is a common measure used to judge the success of a "profile-modification" treatment. For convenience in the following study, we assume that the resistance factor for gelant is equal to one.

The fluid injectivity, I_{io}, in direction i prior to gelant injection can be found by Eq. 3 (Eqs. 3, **4,** and 5 are derived in Appendix D of Ref. **13).**

$$I_{,,} = \frac{q_{io}}{p_w - p_e} = \frac{\theta_i h k_i}{141.2 \mu_w \ln\left(\frac{r_e}{r_w}\right)} \qquad (3)$$

where

h = thickness of the net pay, ft

P_e = pressure at the outer boundary, psi

P_w = pressure at the injection well, psi

q_{io} = total injection rate before gelant placement, B/D

μ_w = water viscosity, cp

The fluid injectivity, I_i, in direction i after gelation can be found by Eq. 4.

$$I_i = \frac{q_i}{p_w - p_e} = \frac{\theta_i h k_i}{141.2\mu_w \left[F_{rr} \ln\left(\frac{r_{pi}}{r_w}\right) + \ln\left(\frac{r_e}{r_{pi}}\right) \right]} \tag{4}$$

where

F_{rr} = residual resistance factor (brine mobility before gelant injection divided by brine mobility after gelation)

q_i = total brine injection rate after gel forms, **B/D**

The overall injectivity ratio, I/I_o, or the ratio of the total brine injection rate after gel forms to the total brine injection rate before gelant injection, is given by Eq. 5.

$$\frac{I}{I''} - \frac{\sum_i q_i}{\sum q_{io}} = \frac{\sum_i \frac{k_i}{F_{rr} \ln\left(\frac{r_{pi}}{r_w}\right) + \ln\left(\frac{r_e}{r_{pi}}\right)}}{\sum_i \frac{k_i}{\ln\left(\frac{r_e}{r_w}\right)}} \tag{5}$$

Comparison of Linear Flow with Anisotropic Radial Flow

The primary question to be answered in this work is, how anisotropic must an unfractured reservoir be to allow gelant placement and profile modification to approach that associated with a linear flow geometry? Fig. 3 can be used to answer this question. Figs. 3a through 3c plot injectivity ratio, I_i/I_{io}, vs. permeability ratio for three cases of gel residual resistance factor. The case where $F_{rr}=2$ corresponds to a

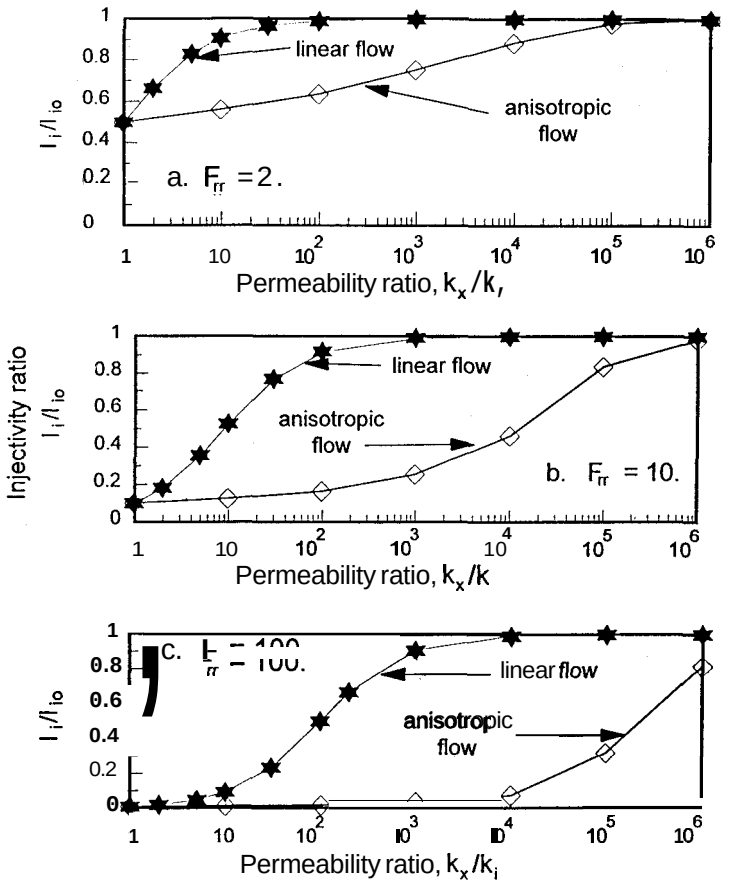

FIG. 3. Comparison of injectivity ratio for linear flow and anisotropic radial flow when r_{px} = 50 ft.

"weak" gel; the F_{rr} = 100 case represents a fairly "strong" gel; while the F_{rr} = 10 case can be associated with a gel of intermediate strength.

Because linear flow has been shown to provide the most desirable profile modification results,[4] this case will be used as a base case for comparison with profile modification in anisotropic systems. In these comparisons, we assume that the gelant resistance factor is equal to 1 during gelant placement. In Fig. 2 and Ref. **4,** the case

where $F_r=1$ was shown to provide the best result during gelant placement (i.e., minimum gelant penetration into low-permeability zones and maximum gelant penetration into high-permeability zones).

After gel placement, profile modification can be assessed using the injectivity ratios, I_i/I_{io}, in Fig. 3. This ratio is the brine injectivity in direction i after gel placement divided by that before gel placement. To illustrate the utility of Fig. 3, consider an anisotropic zone that is 10 times more permeable in the x-direction than in the i-direction (i.e., $k_x/k_i=10$). For a gel with $F_{rr}=2$, Fig. 3a indicates that in the x-direction, 50% of the original injectivity will remain after the gel treatment. In the i-direction (where $k_x/k_i=10$), 56.5% of the original injectivity will remain after the gel treatment. Ideally, we want the gel treatment to reduce injectivity in the x-direction by a large factor, while having little effect on injectivity in the i-direction. Unfortunately, in our example, the gel treatment improved the flow profile only slightly while reducing injectivity by about 50% in both the x-direction and the i-direction. The benefit from this minor redistribution of fluid flow is unlikely to offset the loss of driving force (injectivity) for displacing oil in the i-direction.

For comparison, consider a similar gel treatment in linear flow (e.g., a fractured well) instead of anisotropic radial flow. Again, we assume that $k_x/k_i=10$ and $F_{rr}=2$. The linear flow case could be a fracture that cuts through two zones—Zone x with permeability k_x, and Zone i with permeability k_i. From the solid curve in Fig. 3a, in Zone x (where $k_x/k_i=1$), 50% of the original injectivity will remain after the gel treatment. However, in Zone i (where $k_x/k_i=10$), 91% of the original injectivity will remain after the gel treatment. Thus, in linear flow, the gel treatment results in a substantial improvement in the flow profile and a relatively small amount of damage (9% injectivity loss) in Zone i. In contrast, to achieve this same result in anisotropic radial flow, k_x/k_i must be 10,000.

Using Figs. 3a-3c, similar analyses can be performed for different gel residual resistance factors. These analyses show that k_x/k_i must be greater than 1,000 (and usually greater than 10,000)before anisotropy can be exploited to achieve a satisfactory gel placement in unfractured wells. We doubt that any unfractured reservoirs exist with this degree of anisotropy. In contrast, in wells and reservoirs where anisotropic flow is due to fractures, the linear flow geometry and the extreme permeability contrast between the fracture and the porous rock can aid gel placement substantially.[4,8,12]

Effect of Distance of Gelant Penetration

In the previous section, the gelant penetrated 50 ft in the x-direction. Using Fig. 4, we examined the sensitivity of profile modification to the distance of gelant penetration. Figs. 4a through 4c plot injectivity ratio vs. permeability ratio for different radii of gelant penetration in the x-direction (r_{px}). Analysis of these figures reveals that for r_{px} values greater than 5 ft, very large k_x/k_i values (typically greater than 1,000) are needed to attain a satisfactory profile modification. Figs. 4b and 4c suggest that in some circumstances, an acceptable profile modification could be attained if $r_{px} \leq 1$ ft, $k_x/k_i \geq 10$, and $10 \leq F_{rr} \leq 100$. Of course, these treatments would involve very small gelant volumes and their effects would be confined to the region very near the wellbore.

Careful consideration of Ref. 4 and Eqs. 2 through 4 reveals that the conclusions reached in the preceding sections and figures apply to areal anisotropy in vertically stratified reservoirs with noncommunicating layers as well as to individual strata.

Conclusions for Model 1

1. During unconfined gelant injection, a satisfactory placement for the gelant is far more likely to occur in a linear flow geometry than in an anisotropic radial flow geometry.
2. As we expected, the injectivity after gelation decreases as the value of residual resistance factor and the distance of gelant penetration increase.
3. For a given permeability ratio, the degree of gelant penetration, $(r_{pi}-r_w)/(r_{px}-r_w)$, increases with increased resistance factor.
4. For the range of permeability variations investigated ($k_x/k_i \leq 10^6$), the degree of gelant penetration is insensitive to resistance factor for $F_r \geq 100$.
5. The above conclusions also apply to heterogeneous reservoirs with multiple noncommunicating layers.

ANALYSIS USING MODEL 2

In Model 1, a uniform pressure drop was applied across a radial reservoir that was areally anisotropic with respect to permeability. In Model 2, the radial reservoir

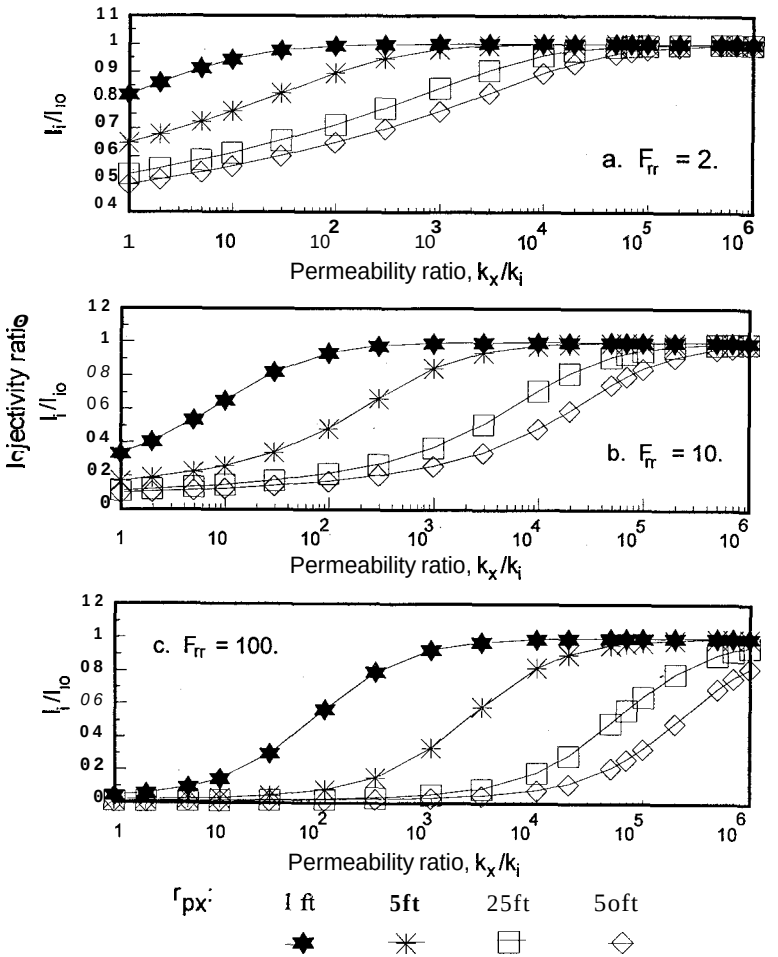

FIG. **4.** Injectivity ratios in anisotropic radial flow for different radii of gelant penetration.

was isotropic with respect to permeability, but the pressure drop across the reservoir varied with direction. The pressure distribution was symmetrical about both the x-axis and the y-axis, and only the injection well was assigned a constant pressure. The reservoir experienced the largest pressure drop in the x-direction while the smallest pressure drop occurred in the y-direction. For many of the results shown in this section (Figs. 5, **7,** and 8), the pressure at the injection wellbore was 3,000 psi, the pressure at the outer boundary in the x-direction was 1,000 psi, and the pressure at the outer boundary in the y-direction was 2,800 psi.

Model Description

Because of the symmetrical pressure distribution, only the first quadrant was considered. To quantitatively describe this model, a pressure distribution was assigned so that the pressure value at any point of the outer boundary was proportional to the angle between the x-axis and the line passing through the injection well (i.e., the origin) and the point considered.

In Model 2, both analytical and numerical methods were used to attack the problem. Since we hoped to perform a reliable sensitivity study, we needed an accurate description of the profile for the gelant front and the pressure distribution. Finite-element and finite-difference methods, which are widely used in large-scale reservoir problems, may not be optimal for this purpose. **A** finite-mesh system may not represent the shape of the gelant front accurately enough, and the superposition technique, which is often incorporated in finite-difference methods, also seems awkward for handling the pressure values along the outer boundary. Therefore, for this problem, we used another numerical method—the Fourier series approximation.[14]

Pressure Profile Before Gel Placement

During brine injection before gel placement or during injection of a gelant with $F_r = 1$, the pressure at any point within the drainage area can be expressed by Eq. **6.** **(Eq.** 6 is derived in Appendix E of Ref. 13.)

$$p = \frac{\frac{m\pi}{4} + n - p_w}{\log\left(\frac{r_e}{r_w}\right)} \log(r) + p_w - \log(r_w) \frac{\frac{m\pi}{4} + n - p_w}{\log\left(\frac{r_e}{r_w}\right)} + \sum_{j=1,3,5,\ldots}^{\infty} \left[\frac{2m}{\pi j^2 \left(r_w^{4j} r^{-2j} - r_e^{2j}\right)} r^{2j} + \frac{2m}{\pi j^2 \left(r_w^{-4j} r_e^{2j} - r_e^{-2j}\right)} r^{-2j} \right] \cos(2j\theta) \quad (6)$$

where

m = slope of the linear distributions at the outer boundary

n = the pressure at the intersecting point of the x-axis and the outer boundary, psi

Using Eq. **6,** pressure profiles were generated for the case where the pressure drop was 10 times greater in the x-direction than in the y-direction ($\Delta p_x/\Delta p_y = 10$). The results (Fig. 5) show that radial flow only existed close to the injection wellbore. The streamlines from the injection well quickly turned to parallel the x-axis as they penetrated into the reservoir. Fluid was forced to flow away from the y-axis. Thus, the region at the outer boundary near the y-axis was not swept by the injected fluid.

Fig. 6 shows gelant-front profiles for different pressure-drop ratios when gelant reached the outer boundary in the x-direction. Fig. 6 was generated by following several streamlines from the injection well using an appropriate timestep. As shown in Appendix F of Ref. 13, a Fortran program was used to execute this procedure. The program also solves for the mathematical expression of the gelant front using a least-squares fit.

In Fig. 6, the gelant-front profiles appear to be insensitive to pressure-drop ratio for $\Delta p_x/\Delta p_y$ values greater than 100. This result is intuitively incorrect and contrasts with the results shown in Fig. 1. These incorrect profiles probably resulted from numerical limitations associated with Model 2. Since we assigned a constant pressure drop in the x-direction (1,000 psi), as the $\Delta p_x/\Delta p_y$ increased, the change of pressure at any point at the outer boundary decreased to small values. Consequently, the profiles for the gelant fronts appear to be insensitive to the higher values of pressure-drop ratio. (We will elaborate on the numerical limitations of our methods later.) We feel that our results using $\Delta p_x/\Delta p_y$ values of 10 or less are probably reliable. However, the results for $\Delta p_x/\Delta p_y$ values greater than 100 are undoubtedly unreliable.

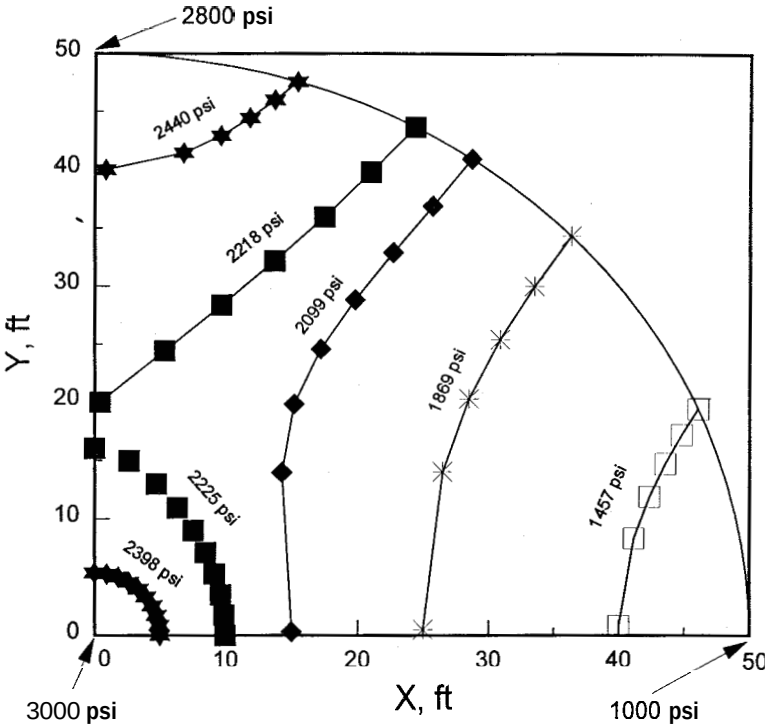

FIG. 5. Pressure profile during brine injection before gel placement when $\Delta p_x/\Delta p_y = 10$.

Pressure Profile After Gel Forms

Pressure profiles during brine injection after gelation were determined for different distances of gelant penetration. We focused on the case where the pressure drop in the x-direction was 10 times that in the y-direction.

Fig. 7 shows the pressure profiles for three values of residual resistance factor ($F_{rr}=2$, $F_{rr}=10$, and $F_{rr}=100$). In these cases, the gel extended 5 ft from the wellbore in the x-direction. An analytical method (described in Appendix G of Ref. 13) was used to determine the pressure profiles. A comparison of the equipotential lines in

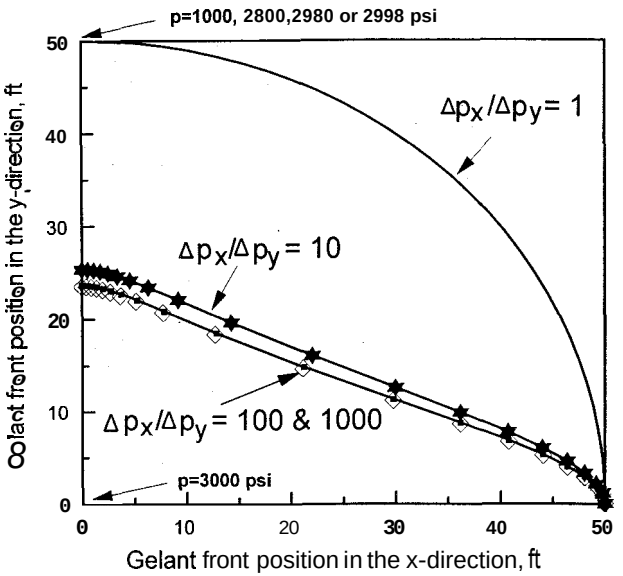

FIG. 6. Plan view of the gelant front in the first quadrant when gelant reached the outer boundary in the x-direction.

Figs. 5 and 7 reveals that the gel treatments (with $F_{rr}=2$, $F_{rr}=10$, or $F_{rr}=100$) did not significantly improve the areal flow profiles.

For comparison, Fig. 8 shows the pressure profiles for the three typical values of residual resistance factor when gelant extended to the outer boundary in the x-direction. A Fourier-approximation method was used to establish the pressure profiles, and a Gaussian elimination technique was used to solve the simultaneous-linear-equation set. Details of the solution can be found in Appendix H of Ref. 13. In Fig. 8, as F_{rr} increases, the equipotential lines bend upward toward the y-axis in the zone swept by the gelant while bending downward toward the x-axis in the zone not swept by the gelant. In this case, the injected fluid is diverted to the y-axis in the zone swept by the gelant. However, outside of the gel-treated region, a close comparison with Fig. 5 reveals no significant improvement in the areal flow profile.

Based on the above analysis, a satisfactory placement for the gelant did not occur for the case where the pressure drop ratio, $\Delta p_x/\Delta p_y$, was 10.

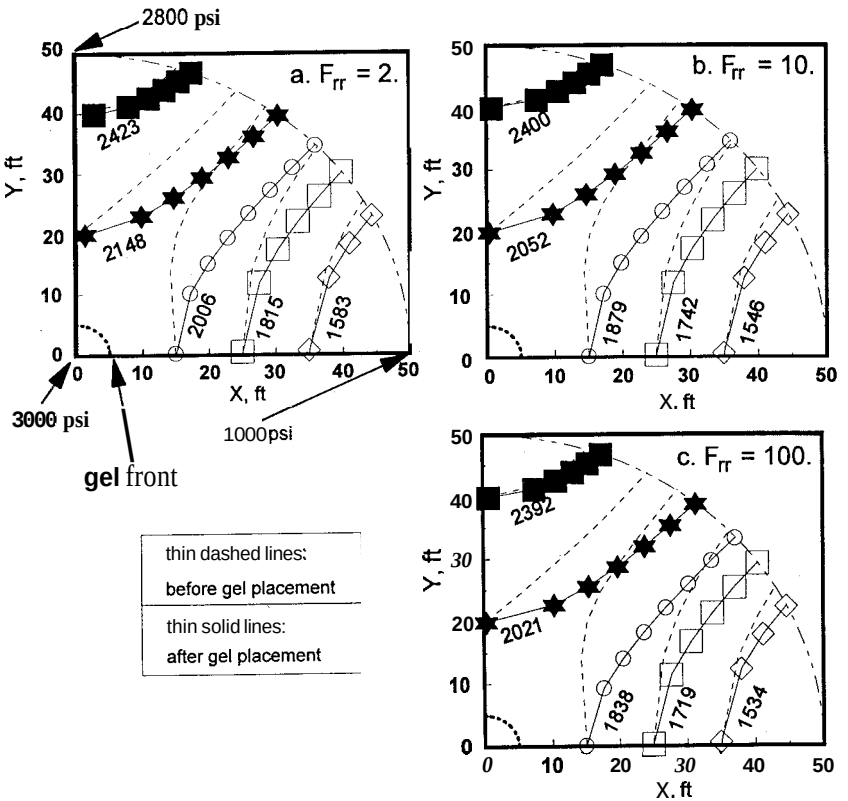

FIG. 7. Pressure profiles during brine injection after gel placement when r_{px} = 5 ft and $\Delta p_x/\Delta p_y$ = 10. Pressures (in psi) are given for each solid equipotential curve.

Limitations Associated with Using Numerical Methods in Model 2

Theoretically, Fourier approximation can describe pressure distributions very well. However, in practice, this method experiences many problems that are associated with most numerical methods. First, using finite terms to approximate the infinite series results in a truncation error. Second, underflow or overflow problems during computations also reduce the accuracy of the calculation. The combined errors may

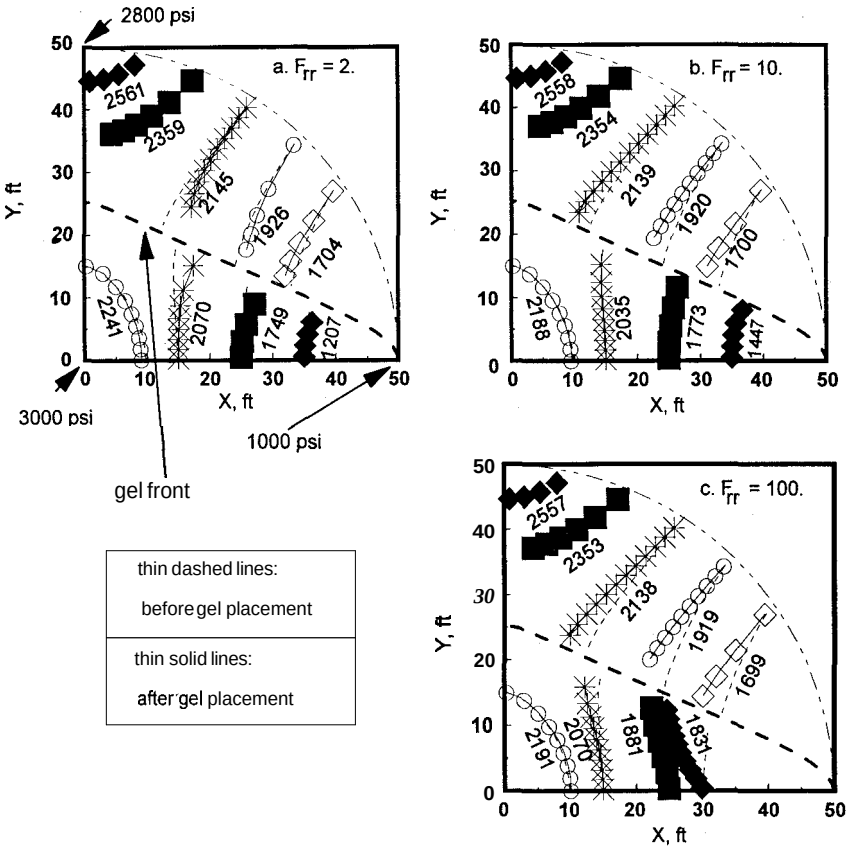

FIG. 8. Pressure profiles during brine injection after gel placement when r_{px} = 50 ft and $\Delta p_x/\Delta p_y$ = 10. Pressures (in psi) are given for each solid equipotential curve.

propagate and distort the results. We also found that the mathematical expression for the gelant-front profile that was generated by the least-squares fit did not exactly match the actual profile. We also noted that injectivity losses were difficult to evaluate quantitatively using numerical methods with Model 2. Finally, numerical limitations precluded our investigation of cases where $\Delta p_x/\Delta p_y$ values were greater than 100.

HORIZONTAL WELLS

How does our analysis impact gel placement in horizontal wells? In horizontal wells without fractures, vertical permeability variations are usually more extreme than directional horizontal permeability variations in vertical wells. Therefore, we might expect flow from horizontal wells to be more anisotropic than that from vertical wells. However, this circumstance is usually not sufficient to change the basic finding of this paper—that oil zones must be protected during gel placement in unfractured wells. To explain, the wellbore diameter in a horizontal well is generally small compared to the thickness of a given zone. Thus, flow from the well will be more or less radial until the gelant front reaches the upper and/or lower boundaries of the zone. After that point, flow may become linear. However, previous work[4] has shown that the gel closest to the wellbore has the greatest impact on the effectiveness of the gel treatment. Thus, the most important part of the gel placement is dominated by radial flow.

CONCLUSIONS

1. During unconfined gelant injection, a satisfactory placement for the gelant is far more likely to occur in a linear flow geometry than in an anisotropic radial flow geometry.
2. As we expected, the injectivity after gelation decreases as the value of residual resistance factor and the distance of gelant penetration increase.
3. For a given permeability ratio, the degree of gelant penetration, $(r_{pi}-r_w)/(r_{px}-r_w)$, increases with increased resistance factor.
4. For the range of permeability variations investigated ($k_x/k_i \leq 10^6$), the degree of gelant penetration becomes insensitive to resistance factor for $F_r \geq 100$.
5. The above conclusions also apply to heterogeneous reservoirs with multiple noncommunicating layers.
6. In an isotropic radial reservoir where the pressure drop was 10 times greater in the x-direction than in the y-direction ($\Delta p_x/\Delta p_y = 10$), the anisotropy induced did not allow a gel treatment to significantly improve the areal flow profile in the reservoir.

ACKNOWLEDGEMENTS

We gratefully acknowledge financial support from the U.S. Department of Energy, the State of New Mexico, ARCO Exploration and Production Technology Co., British Petroleum, Chevron Petroleum Technology Co., Conoco Inc., Exxon Production Research Co., Marathon Oil Co., Mobil Research and Development Corp., Phillips Petroleum Co., Texaco, and UNOCAL.

NOMENCLATURE

F_r = resistance factor (brine mobility before gelant divided by gelant mobility)
F_{rr} = residual resistance factor (brine mobility before gelant injection divided by brine mobility after gelation)
h = thickness of the net pay, ft
I = injectivity, B/D-psi
I_i = injectivity in direction i, B/D-psi
I_o = initial injectivity, B/D-psi
I_{io} = initial injectivity in direction i, BID-psi
j = counter in Eq. 6
k_i = permeability in radial direction i, md
k_x = permeability in the most-permeable direction (x-direction), md
k_y = permeability in the least-permeable direction (y-direction), md
m = slope of the linear pressure distribution for the outer boundary
n = pressure at the intersection point of the outer boundary and the x-axis, psi
p = pressure, psi
p_e = pressure at the outer boundary, psi
p_w = pressure at the injection well, psi
q_i = total brine injection rate after gel forms, B/D
q_{io} = total brine injection rate before gelant placement, B/D
r = radius, ft
r_e = radius of the outer drainage boundary, ft
r_{pi} = distance of gelant penetration in radial direction i, ft
r_{px} = distance of gelant penetration in the x-direction, ft
r_w = radius of the injection wellbore, ft

θ = the angle between the x-direction and the considered direction

θ_i = the angle between radial direction i and the x-direction

μ_w = water viscosity, cp

ϕ_i = porosity in radial direction i

REFERENCES

1. Sydansk, R.D. and Moore, P.E.: "Gel Conformance Treatments Increase Oil Production in Wyoming," *Oil & Gas J.* (Jan. 20, 1992) 40-45.

2. Moffitt, P.D.: "Long-Term Production Results of Polymer Treatments on Producing Wells in Western Kansas," *Journal of Petroleum Technology* (April 1993) 356-362.

3. Seright, R.S. and Liang, J.: "A Survey of Field Applications of Gel Treatments for Water Shutoff," paper SPE 26991 presented at the 1994 SPE Permian Basin Oil & Gas Recovery Conference, Midland, TX, March 16-18.

4. Seright, R.S.: "Placement of Gels to Modify Injection Profiles," paper SPE/DOE 17332 presented at the 1988 SPE/DOE Symposium on Enhanced Oil Recovery, Tulsa, OK, April 17-20.

5. Seright, R.S.: "Effect of Rheology on Gel Placement," *SPE Reservoir Engineering* (May 1991), 212-218; *Transactions* AIME **291.**

6. Seright, R.S.: "Impact of Dispersion on Gel Placement for Profile Control," *SPE Reservoir Engineering* (Aug. 1991) 343-352.

7. Liang, J., Lee, R.L., and Seright, R.S.: "Placement of Gels in Production Wells," *SPE Production & Facilities* (Nov. 1993) 276-284; *Transactions* AIME **295.**

8. Seright, R.S.: "Gel Placement in Fractured Systems," *SPE Production & Facilities* (Nov. 1995), 241-248.

9. Lake, L.W.: "The Origins of Anisotropy," *Journal of Petroleum Technology* (April 1988) 395-396.

10. Elkins, L.F. and Skov, A.M.: "Determination of Fracture Orientation from Pressure Interference," *Journal of Petroleum Technology* (Dec. 1960) 301-304; *Trans.*, AIME, **219.**

11. Ramey, H.J.: "Interference Analysis for Anisotropic Formations—A Case History," *Journal of Petroleum Technology* (Oct. 1975) 1290-1298; *Trans.*, AIME, **259.**

12. Seright, R.S.: "A Comparison of the Use of Gelants and Preformed Gels for Conformance Control in Fractured Systems," paper SPE 35351 presented at the 1996 SPE/DOE Symposium on Improved Oil Recovery, Tulsa, OK, April 21-24.

13. Seright, R.S.: "Improved Techniques for Fluid Diversion in Oil Recovery Processes," second annual report (DOE/BC/14880-10), Contract No. DE-AC22-92BC14880, U.S. DOE (March 1995) 161-195.

14. Muskat, M.: *The Flow of Homogeneous Fluids Through Porous Media,* McGraw-Hill Book Co. Inc., New York (1937) 164-165.